

# Structural Behavior of a Homologous Series of Thermotropic Polyesters with Biphenyl Mesogen under Hydrostatic Pressure

Yoji Maeda\*<sup>†</sup> and Junji Watanabe<sup>‡</sup>

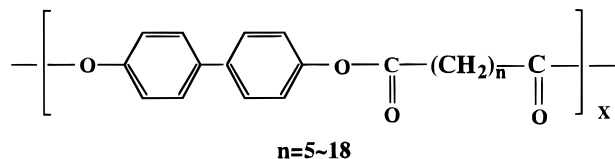
National Institute of Materials and Chemical Research, 1-1 Higashi, Tsukuba, Ibaraki 305, Japan, and Department of Polymer Chemistry, Tokyo Institute of Technology, Ookayama, Meguro-ku, Tokyo 152, Japan

Received January 17, 1997; Revised Manuscript Received May 5, 1997<sup>®</sup>

**ABSTRACT:** The structural behavior of a homologous series of thermotropic (4,4'-dihydroxybiphenyl)-alkanedioic acid polyesters (PB-*n*, *n* indicates the number of methylene units in the spacer) with alkylene spacers ranging from *n* = 10 to *n* = 18 was studied using wide-angle X-ray diffraction under hydrostatic pressures up to 300 MPa. PB-10 shows an enantiotropic transition of crystal (*K*<sub>1</sub>)–smectic H (*S*<sub>H</sub>)–isotropic phase (I) in the whole pressure region. The long *d* spacing of the low-angle reflection for the *K*<sub>1</sub> phase is constant in the crystalline state and then shrinks discontinuously by about 2.4 Å at the *K*<sub>1</sub>–*S*<sub>H</sub> transition, while the *d* spacings of wide-angle reflections change gradually with temperature. Both *d* spacings of the *K*<sub>1</sub> crystal are slightly deformed by applying pressure. In PB-12 the same transition process is observed in the pressure region below 100 MPa, while the smectic B(*S*<sub>B</sub>) phase is induced in place of the *S*<sub>H</sub> phase under a higher pressure. On the other hand, PB-14–PB-18 polyesters exhibit a crystal polymorph (*K*<sub>2</sub>) between the *K*<sub>1</sub> and *S*<sub>H</sub> phases. In these polyesters, the long *d* spacing increases gradually by about 1–2 Å with temperature during a broad *K*<sub>1</sub>–*K*<sub>2</sub> transition. Then a longer *d* spacing of the *K*<sub>2</sub> phase shrinks rapidly at the *K*<sub>2</sub>–*S*<sub>H</sub> transition on heating. It is found that both *K*<sub>1</sub> and *K*<sub>2</sub> crystals are deformed substantially in the molecular chain direction by applying pressure, in contrast to a slight change in the *d* spacing of the *S*<sub>H</sub> phase. The structural behavior during the *K*<sub>1</sub>–*K*<sub>2</sub>–*S*<sub>H</sub>–I transition process of PB-14–PB-18 polyesters is observed reversibly in the whole pressure region.

## Introduction

Semiflexible homopolyesters having rigid and flexible segments in a repeating unit show interesting thermal properties because their transition temperatures can be controlled by modifying the chemical composition in the flexible segment.<sup>1–4</sup> Asrar et al.<sup>5</sup> reported the synthesis and properties of a homologous series of (4,4'-dihydroxybiphenyl)alkanedioic acid polyester, abbreviated as PB-*n*, *n* indicating the number of methylene units in the flexible spacer. PB-*n* polyesters are prepared from 4,4'-dihydroxybiphenyl as a mesogen and aliphatic dibasic acids containing 5–18 methylene units as a flexible spacer. The chemical structure of PB-*n* polyesters is shown as follows.



Structure and properties of PB-*n* polyesters at atmospheric pressure have been studied in the last decade.<sup>6,7</sup> The thermotropic polyesters exhibit a remarkable odd–even effect, and PB-*n* polyesters having an even number of methylene units show a smectic H (*S*<sub>H</sub>) phase in a relatively broad temperature region between the crystal (*K*<sub>1</sub>) and the isotropic melt (I). The *S*<sub>H</sub> phase is identified as a tilted smectic phase. The relation between the transition temperature and the number of methylene units *n* of PB-*n* polyesters indicates that both linear curves of *T*<sub>K–S</sub> vs *n* and *T*<sub>S–I</sub> vs *n* relations are bent out at *n* = 12. Also the *T*<sub>S–I</sub> vs *n* relation is extrapolated to

intersect the *T*<sub>K–S</sub> vs *n* curve at about *n* = 30.<sup>8</sup> This implies that the *S*<sub>H</sub> phase appears no longer in PB-*n* polyesters having very long spacers (*n* > 32). The anchoring effect of rigid dihydroxybiphenyl units as mesogen is suggested to be overwhelmed by conformational disordering in flexible spacers of methylene units with *n* > 32.

The effect of pressure on the phase transition of low-molar mass liquid crystals<sup>9–13</sup> and thermotropic polymers<sup>14–17</sup> have been studied on the theoretical and experimental points of view. The authors reported the phase diagrams of PB-7, PB-8,<sup>18</sup> and PB-12<sup>19,20</sup> polyesters under hydrostatic pressure. Typical transitions of *K*<sub>1</sub>–nematic (N)–I for PB-7 and *K*<sub>1</sub>–*S*<sub>H</sub>–I for PB-8 were clearly observed at pressures up to 300 MPa, respectively. Also, in the case of PB-12, the same transition behavior as one of PB-8 is observed in the pressure region up to 90–100 MPa. However, a quite different change in wide-angle X-ray diffraction (WAXD) profiles is observed at the *K*<sub>1</sub>–*S*<sub>H</sub> transition under higher pressures, indicating the appearance of a pressure-induced mesomorphism.<sup>19,20</sup> The *S*<sub>H</sub> phase in the lower pressure region alters to form a new smectic phase at high pressures above 100 MPa. According to Gray and Goodby's definition of smectic liquid crystals, the *S*<sub>H</sub> phase is a smectic mesophase in which the molecules have their axes tilted with respect to the normal to the layer plane.<sup>21</sup> The new smectic phase is suggested to be the smectic–B (*S*<sub>B</sub>) phase because the molecules are arranged with their long axes perpendicular to the layer plane in a hexagonal close-packed array. The phase diagram determined by high-pressure WAXD measurement indicates the stable regions for the *K*<sub>1</sub> crystal, *S*<sub>H</sub> phase, *S*<sub>B</sub> phase, and the isotropic phase.<sup>20</sup> The unusual phenomenon on the PB-12 polyester encouraged us to study further the effect of pressure on the thermal and structural behavior of a homologous series of PB-*n* polyesters having longer alkylene spacers. The thermal behavior of PB-10–PB-18 polyesters is already studied

\* Author for correspondence.

<sup>†</sup> National Institute of Materials and Chemical Research.

<sup>‡</sup> Tokyo Institute of Technology.

<sup>®</sup> Abstract published in *Advance ACS Abstracts*, June 15, 1997.

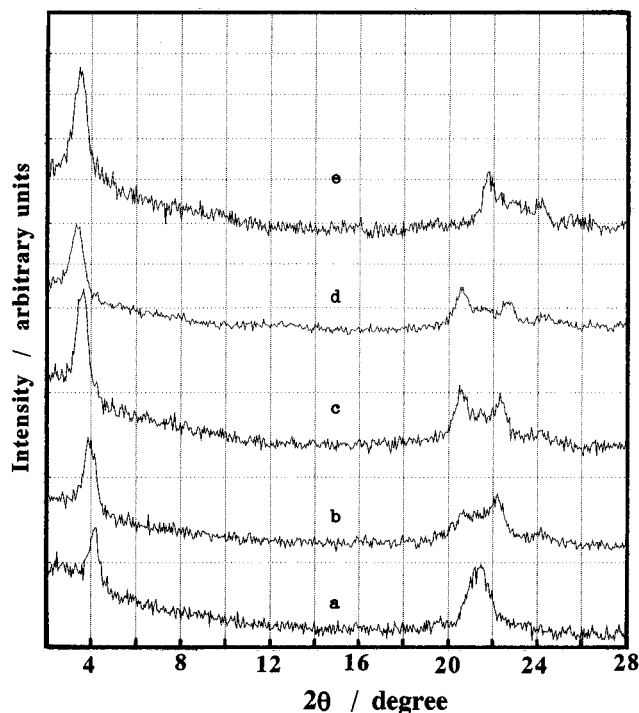


**Figure 1.** WAXD profiles of a homologous series of PB-*n* crystals at 23 °C under atmospheric pressure: (a) PB-10; (b) PB-12; (c) PB-14; (d) PB-16; (e) PB-18.

by a high-pressure DTA apparatus, and phase diagrams of these polyesters are constructed in a pressure region up to 400 MPa.<sup>8</sup>

In this study, the effect of pressure on the structural behavior accompanied with phase transitions of these PB-*n* polyesters has been investigated by using a WAXD apparatus equipped with a high-pressure sample vessel and PSC-MCA data acquisition system.

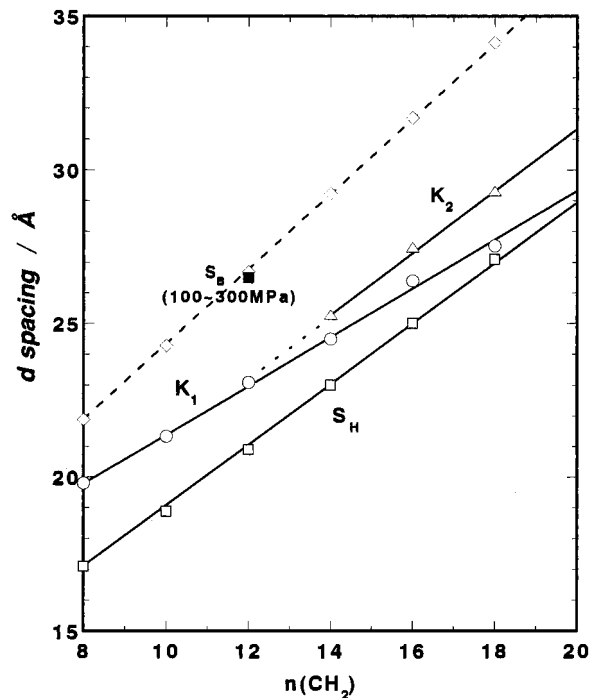
## Experimental Section

**Materials.** Polyesters were synthesized by melt condensation (transesterification) of 4,4'-dihydroxybiphenyl and aliphatic dibasic acids at about 250 °C and by interfacial polycondensation. The synthesis of PB-*n* polyesters is described elsewhere.<sup>6,7</sup> The inherent viscosities of the samples were determined by an Ubbelohde viscometer at 25 °C using 0.5 g dL<sup>-1</sup> solution in a 60/40 mixture by weight of phenol and tetrachloroethane. Inherent viscosities of PB-10, PB-12, and PB-14 were 0.60, 0.75, and 0.72 dL g<sup>-1</sup>, respectively, but both viscosities of PB-16 and PB-18 could not be measured because of low solubility in the mixed solvent.

**WAXD Measurement under High Pressure.** The X-ray structural behavior of PB-*n* polyesters has been observed under hydrostatic pressures up to 300 MPa by using a WAXD apparatus equipped with a high-pressure X-ray vessel described elsewhere.<sup>22,23</sup> Dimethylsilicone oil with low viscosity (10 centistokes) was used as a pressure medium. X-ray measurements of the samples were performed at a scanning rate of 1–2 °C/min in a temperature region between room temperature and 300 °C under various pressures. The pressure was monitored by a manganin gauge, which was calibrated by a Heise bourdon gauge.

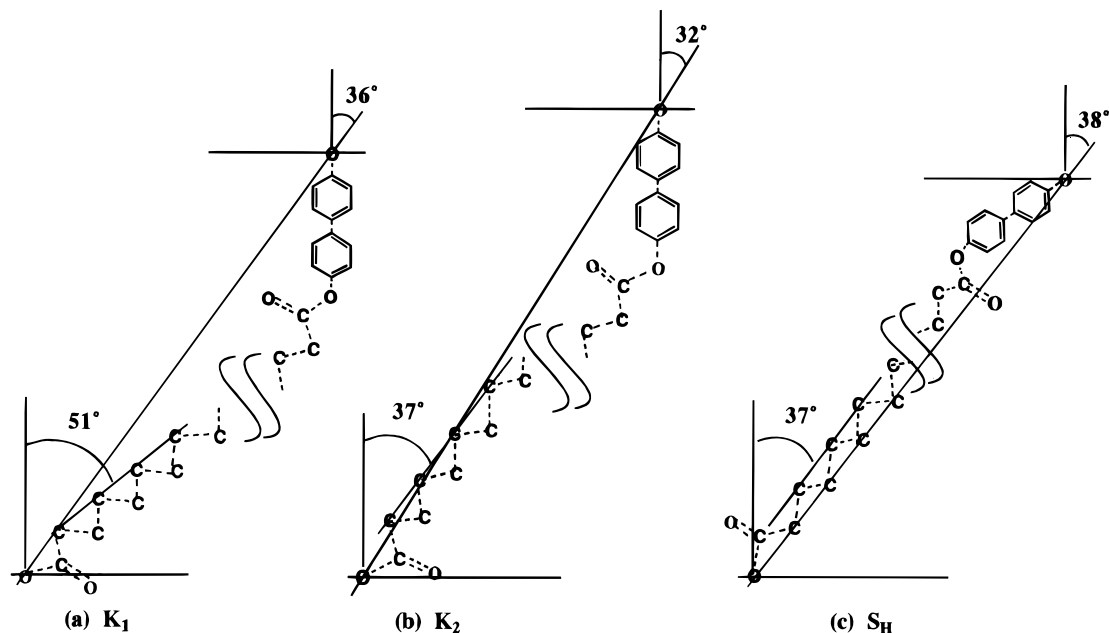
## Results and Discussion

Figure 1 shows the typical WAXD patterns at 23 °C and atmospheric pressure of a homologous series of PB-*n* polyesters with alkylene spacers ranging from *n* = 10 to *n* = 18. Strong reflections are observed at a low angle of  $2\theta \approx 4^\circ$  and wide angles between  $2\theta \approx 20^\circ$  and  $24^\circ$ . The diffraction peak at small  $2\theta$  shifts to lower angles with *n*, indicating an increase of molecular length



**Figure 2.** Relation of the *d* spacing of the low-angle reflection to *n* (number of methylene units in the spacer) of the K<sub>1</sub>, K<sub>2</sub>, and S<sub>H</sub> phases of PB-*n* polyesters at atmospheric pressure. The dotted line shows the relation of the calculated extended length of the repeating unit to the number of methylene units in the spacer.

in the chain direction. At the same time, the X-ray patterns at wide angles clearly show two or three diffraction peaks with increasing *n* of methylene units. Figure 2 shows the relation of the long *d* spacing of the low-angle reflection to *n* for the three phases, i.e., normal crystal (K<sub>1</sub>), crystal polymorph (K<sub>2</sub>), and smectic H (S<sub>H</sub>) phase of PB-*n* under atmospheric pressure. The K<sub>2</sub> crystal polymorph appearing in PB-14–PB-18 is described in a later paragraph. The relation of the calculated extended length of the PB-*n* molecule to *n* is also shown for reference. All the *d* spacing vs *n* curves are approximated to linear relations. It is noted in Figure 2 that a linear curve of the K<sub>1</sub> crystal intersects a curve of the S<sub>H</sub> phase at about *n* ≈ 22. Also, a curve of the K<sub>2</sub> crystal intersects the curve of the K<sub>1</sub> crystal at *n* ≈ 12. Figure 2 explains why the K<sub>2</sub> crystal is not formed in PB-8 and PB-10. All the *d* spacings of the K<sub>1</sub>, K<sub>2</sub>, and S<sub>H</sub> phases, except of the S<sub>B</sub> phase, are smaller than the calculated extended length of the PB-*n* molecule arranged in all-*trans* conformation. From the data of the observed *d* spacing and calculated extended length in Figure 2, the angle between the PB-*n* molecule and its layer normal can be estimated for K<sub>1</sub>, K<sub>2</sub>, and S<sub>H</sub> phases of these polyesters. This angle is varied from 29° in PB-10 to 36° in PB-18 for the K<sub>1</sub> crystal, and from 30° in PB-14 to 32° in PB-18 for the K<sub>2</sub> crystal, while the angle for the S<sub>H</sub> phase is approximately constant at 38–39°, independent of *n*. In addition, the incremental increase of the long *d* spacing per methylene unit is evaluated from the gradient of each *d* vs *n* curve of the K<sub>1</sub>, K<sub>2</sub>, and S<sub>H</sub> phases: it is 0.79 Å for the K<sub>1</sub> phase and 1.01 Å for the K<sub>2</sub> and S<sub>H</sub> phases. These data are smaller than the projected length of a methylene unit along the chain direction, 1.26 Å, indicating that the alkylene spacer makes an angle with respect to the layer normal. The angle between the methylene units in the spacer and the layer normal is estimated to be 51° for



**Figure 3.** Tentative model of molecular arrangements for the  $K_1$  and  $K_2$  crystals and smectic H phase of PB-18. For convenience, the polymer chains in the all-*trans* conformation are postulated.

the  $K_1$  crystal,  $37^\circ$  for the  $K_2$  crystal, and  $37^\circ$  for the  $S_H$  phase. Both values are larger by  $6\text{--}7^\circ$  than the angles reported previously.<sup>6</sup> Figure 3 illustrates a tentative model of molecular arrangements of the  $K_1$ ,  $K_2$ , and  $S_H$  phases of PB-18.

The temperature variation of  $d$  spacings of low- and wide-angle reflections for PB-10–PB-18 polyesters was observed at various pressures up to 300 MPa.

**(1) PB-10.** The structural behavior of the PB-10 polyester shows  $K_1$ – $S_H$  and  $S_H$ –I transitions in the whole pressure region, which coincides completely with the thermal behavior already reported.<sup>8</sup> The pattern and its change of X-ray profiles are substantially the same as those of the  $K_1$ – $S_H$ –I transition of PB-8 under pressure<sup>18</sup> and also of PB-12 at pressures up to 100 MPa.<sup>19,20</sup> Figure 4 shows the temperature variation of both  $d$  spacings estimated from low- and wide-angle reflections of PB-10 under atmospheric pressure (0.1 MPa) and 300 MPa. The long  $d$  spacing is constant in the crystalline state, while  $d$  spacings for wide-angle reflections change continuously with increasing temperature. It is noted that the long spacing is decreased by about  $0.5\text{ \AA}$  by applying pressure at 300 MPa, but the deformation is released at high temperatures just below the  $K_1$ – $S_H$  transition. This fact indicates that the compressional strain in the molecular chain direction can be released by thermal energy at high temperatures. The  $d$  spacing ( $4.0_3\text{ \AA}$ ) of a wide-angle reflection in PB-10 is more sensitive to pressure than the spacing ( $4.2\text{ \AA}$ ) of the other reflection. As one can see in Figure 4, the former changes substantially with temperature, while the latter is slightly dependent of temperature. Accordingly, the  $d$  spacing of the former reflection comes close to the other spacing ( $4.2\text{ \AA}$ ) and they finally merge at a temperature below the  $K$ – $S_H$  transition point. Here the merging point of major wide-angle reflections is defined temporarily as  $T'$ , indicating the midpoint of the  $K_1$ – $S_H$  transition in the lateral direction. So we can discuss phenomenologically the pressure dependence of molecular arrangement during the  $K$ – $S_H$  transition, at least, with respect to the merging point of wide X-ray reflections. In the pretransition region defined between  $T'$  and the  $K_1$ – $S_H$  transition point, the PB-10 crystal

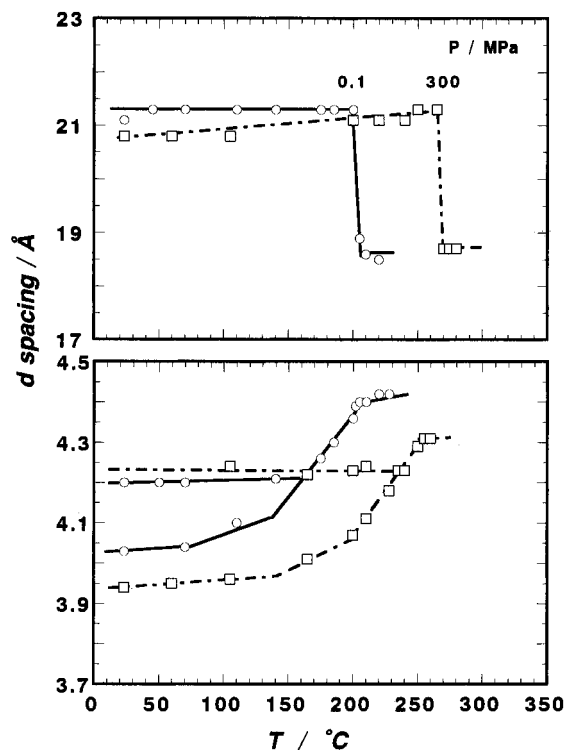


**Figure 4.** Temperature variation in the  $d$  spacing of low- and wide-angle reflections of the PB-10 polyester at 0.1 MPa (○) and 300 MPa (□).

holds a constant long spacing and a variable  $d$  spacing of merged wide-angle reflections. The  $d$  spacing in the lateral direction changes rapidly from  $4.20\text{ \AA}$  to about  $4.40\text{ \AA}$  in this region. When the  $K_1$ – $S_H$  transition occurs at  $204^\circ\text{C}$  and 0.1 MPa, the long  $d$  spacing shrinks discontinuously by about  $2.4\text{ \AA}$  in the chain direction and the lateral spacing changes continuously with temperature. This behavior can be understood by the molecular arrangements reported previously.<sup>6</sup> The long  $d$  spacing ( $18.7\text{ \AA}$ ) of the  $S_H$  phase is slightly deformed and also the spacing of the side packing decreases from  $4.40$  to  $4.31\text{ \AA}$  by applying pressure at 300 MPa. The  $K_1$ – $S_H$ –I transition is completely reversible in the

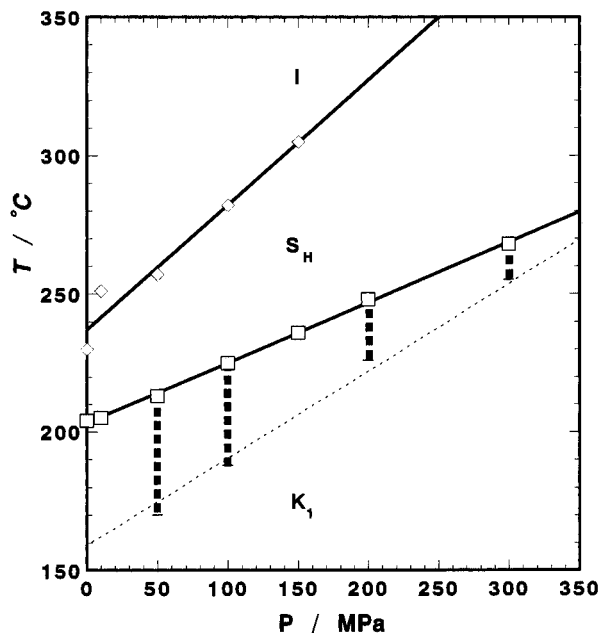


**Figure 5.**  $T$  vs  $P$  phase diagram of the PB-10 polyester. Solid squares show the pretransition region for the  $K_1$ – $S_H$  transition.

whole pressure region. Figure 5 shows the pressure dependence of the transition points of the PB-10 polyester, including the pretransition region between  $T$  and the  $K_1$ – $S_H$  transition point shown as solid squares. All of the transition curves are approximated to linear curves. The  $K_1$ – $S_H$  transition in this study corresponds well to the DTA results of the PB-10 polyester reported previously.<sup>8</sup> It is noteworthy that the pretransition region for the  $K_1$ – $S_H$  transition decreases from 64 °C at 0.1 MPa to 15 °C at 300 MPa, suggesting that rearrangement of molecules during the  $K_1$ – $S_H$  transition occurs sharply at higher pressures.

**(2) PB-12.** The structural behavior of the PB-12 polyester is already reported elsewhere.<sup>20</sup> The pressure-induced mesophase, the  $S_B$  phase, is induced in place of the  $S_H$  phase under hydrostatic pressures above 100 MPa. The long  $d$  spacing increases discontinuously from 22.1 to 26.2 Å during the  $K_1$ – $S_B$  transition at 300 MPa, in contrast to the decrease in  $d$  spacing of about 2.4 Å during the  $K_1$ – $S_H$  transition at low pressures. It is concluded that molecules in the  $S_B$  phase lie almost perpendicular to the smectic layer while molecules in the  $S_H$  phase are tilted to the smectic layer. Figure 6 shows the  $T$  vs  $P$  diagram of the PB-12 polyester. Narrowing of pretransition region with pressure is also observed at the  $K$ – $S_H$  transition in PB-12. Pressure contributes significantly to the sharp pretransition for the  $K_1$ – $S_H$  transition of PB-10 and PB-12 polyesters.

**(3) PB-14.** Transition points of a homologous series of PB- $n$  polyesters generally shift to lower temperature with increasing  $n$  of the methylene units.<sup>8</sup> In PB-14–PB-20 polyesters, the DSC curves show an additional peak at a temperature just below the main peak of the  $K_1$ – $S_H$  transitions. As the number of methylene units increases in the spacer, the additional endothermic peak grows consecutively while the normal peak of the  $K_1$ – $S_H$  transition decreases. Since the transition is apparently a solid-phase transition, the low- and high-temperature crystal phases are labeled as  $K_1$  and  $K_2$ , respectively. The DSC data indicate that the phase transition of  $K_1$ – $K_2$ – $S_H$ – $I$  occurs reversibly under atmospheric pressure.<sup>8</sup>

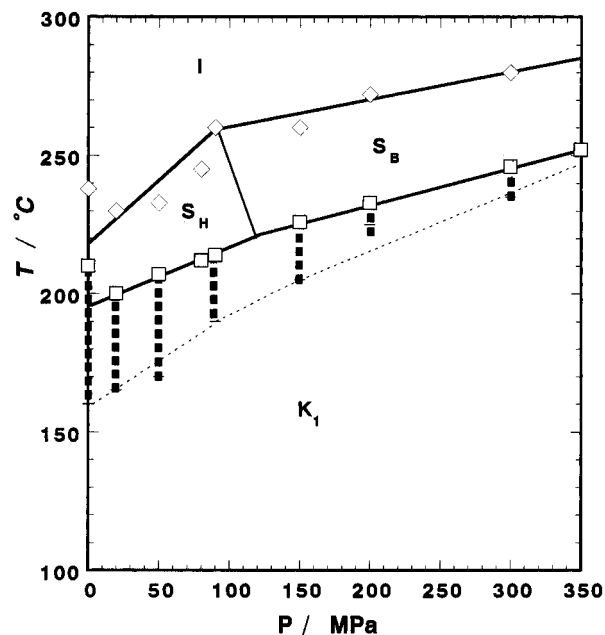


**Figure 6.**  $T$  vs  $P$  phase diagram of the PB-12 polyester. Solid squares are the same as in Figure 5.

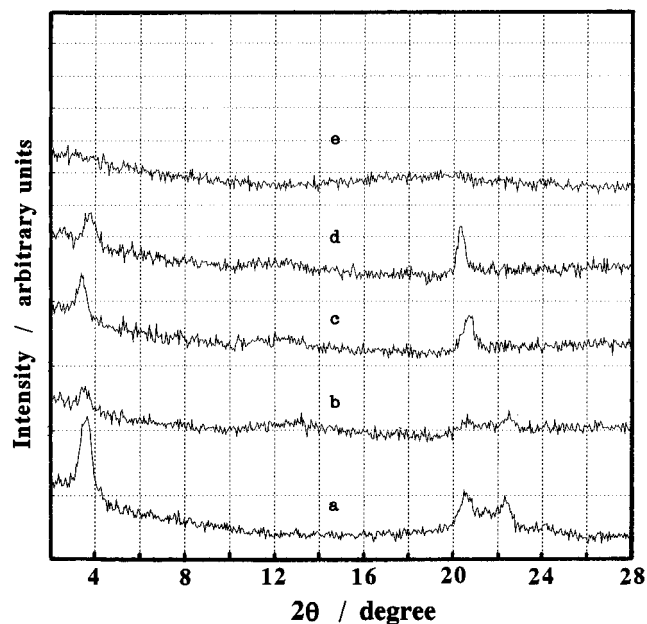


**Figure 7.** WAXD patterns of (a) the  $K_1$  crystal at 22 °C and 0.1 MPa, (b) the  $K_1$  crystal at 22 °C and 100 MPa, (c) the  $K_2$  crystal at 200 °C and 100 MPa, (d) the  $S_H$  phase at 218 °C and 100 MPa, and (e) the isotropic phase at 252 °C and 100 MPa of the PB-14 polyester.

Figure 7 shows the typical WAXD patterns of the  $K_1$ ,  $K_2$ ,  $S_H$ , and isotropic phases of PB-14 polyester at 100 MPa. It is noted that the general feature in the structural behavior of PB-14 is held in the whole pressure region. Figure 8 shows the temperature variation of  $d$  spacings estimated from low- and wide-angle reflections of PB-14 at 100 MPa. It is noteworthy that the  $K_1$ – $K_2$  transition occurs gradually in a wide temperature region of more than 100 °C. The  $K_1$ – $K_2$  transition point is defined here as the end point of the increasing long  $d$  spacing on heating. The long  $d$  spacing of the  $K_1$  phase increases gradually from 24.2 to 25.6 Å, parallel to a gradual change in the  $d$  spacing of the wide-angle reflections. The longer  $d$  spacing of the  $K_2$  phase is constant at temperatures between 185

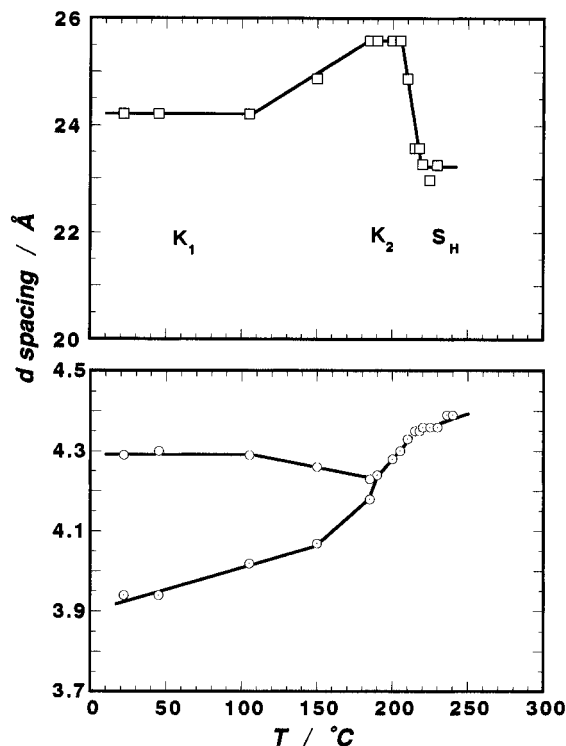


**Figure 8.** Temperature variation in the  $d$  spacing of the low- and wide-angle reflections of the PB-14 polyester at 100 MPa.

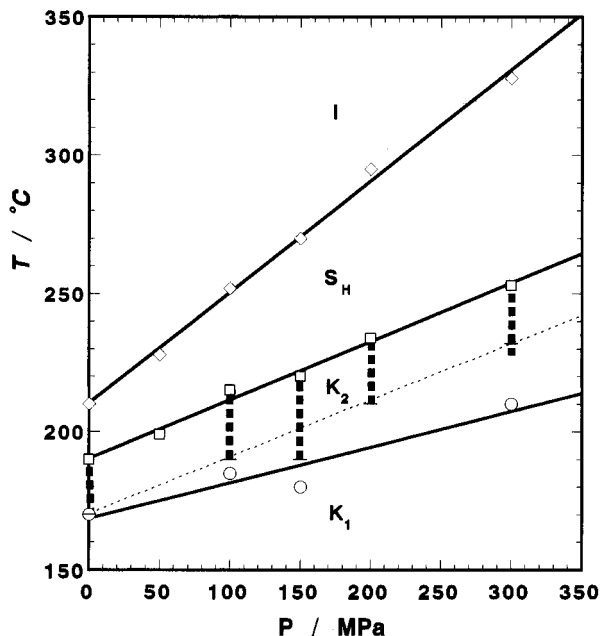


**Figure 9.**  $T$  vs  $P$  phase diagram of the PB-14 polyester. Solid squares are the same as in Figure 5.

and 205 °C, and at the same time the  $d$  spacing of the merged wide-angle reflection increases from 4.24 to 4.30 Å until the  $K_2$ – $S_H$  transition occurs. Characteristics of the  $K_2$  crystal for PB- $n$  ( $n > 14$ ) polyesters is the existence of a longer  $d$  spacing for low-angle reflections and a lateral spacing for merged wide-angle reflections at high temperatures. When the  $K_2$ – $S_H$  transition occurs at temperatures between 205 and 215 °C, the long  $d$  spacing decreases rapidly from 25.6 to 23.3 Å and the lateral spacing changes its steep slope to a steady one. The  $T$  vs  $P$  diagram of the PB-14 polyester is shown in Figure 9. The  $K_1$ – $K_2$ – $S_H$ – $I$  transition process is held in the whole pressure region, but transition points rise linearly with increasing pressure.

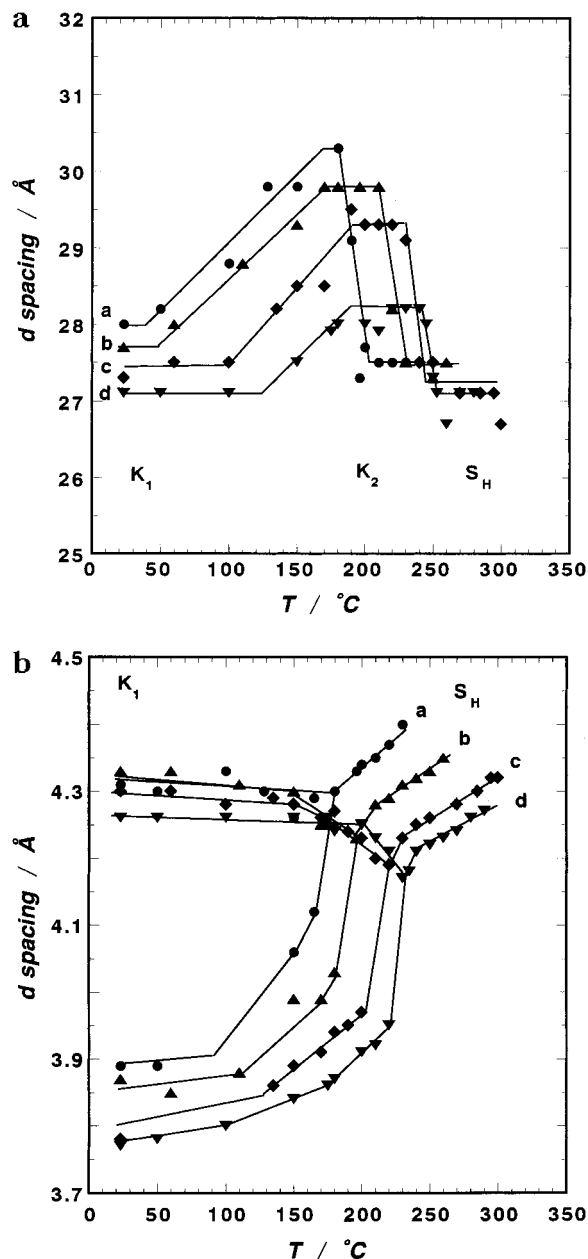


**Figure 10.** Temperature variation in the  $d$  spacing of (a) the low- and (b) the wide-angle reflections of the PB-18 polyester at various pressures: (a) 100 MPa; (b) 200 MPa; (c) 300 MPa; (d) 400 MPa.

**(4) PB-18.** The structural behavior of PB-16 and PB-18 polyesters under pressure is similar to that of PB-14. The structural phenomenon under pressure coincides well with the DTA results by high-pressure thermal analysis.<sup>8</sup> The  $d$  spacings of low- and wide-angle reflections of PB-18 under various pressures are plotted against temperature in Figure 10a,b, respectively. The long  $d$  spacing increases gradually from 27.9 to about 30.3 Å with temperature at 100 MPa, while the major wide-angle reflections are still observed just below the  $K_2$ – $S_H$  transition. It is noted in Figure 10a that both long  $d$  spacings of  $K_1$  and  $K_2$  crystals are deformed substantially by applying hydrostatic pressure, in contrast to a slight change of  $d$  spacing of the  $S_H$  phase. The compressional strain in the molecular chain direction is in the order  $K_2 > K_1 > S_H$ . The larger change in long spacing for the  $K_1$  crystal than for the  $S_H$  phase results in the comparable values of the  $d$  spacing between the phases at high pressures, i.e., 300

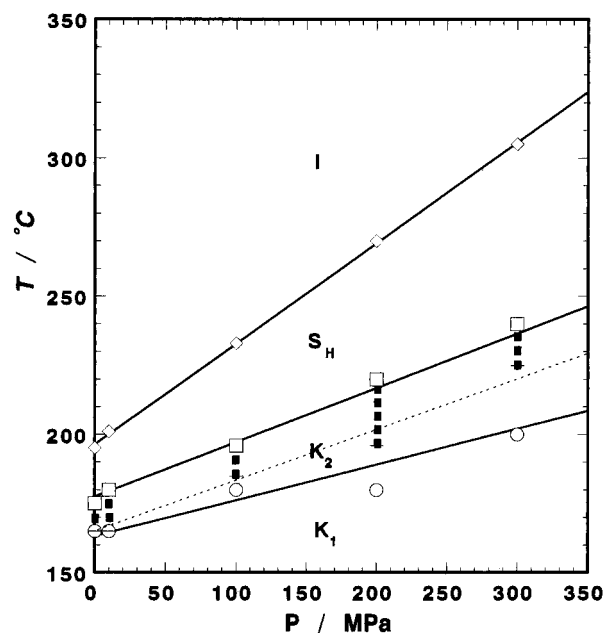


**Figure 11.**  $T$  vs  $P$  phase diagram of the PB-18 polyester. Solid squares are the same as in Figure 5.

and 400 MPa. This indicates that the  $K_1$  crystal has a compressibility larger than that of the  $S_H$  phase in the chain direction, in spite of apparently similar changes in lateral packing. As one can see in Figures 10a,b, the broad temperature region of the  $K_1$ – $K_2$  transition at 0.1 MPa is narrowed with increasing pressure, while the stable regions of the  $K_1$  and  $K_2$  phases tend to broaden with pressure. This is due to the pressure contribution to the sharp  $K_1$ – $K_2$  transition. Figure 11 illustrates the  $T$  vs  $P$  phase diagram of the PB-18 polyester. PB-18 manifests the same phase diagram characteristics as PB-14. In Figures 9 and 11, the  $K_1$ – $K_2$  transition point estimated from the long  $d$  spacing matches with the  $T$  point as the merging point of major wide-angle reflections at 0.1 MPa. When the extension of the  $d$  spacing in the chain direction is completed at the  $K_1$ – $K_2$  transition, major wide-angle reflections merge immediately and lateral packing in the  $K_2$  phase becomes loose with temperature. Afterward the  $K_2$ – $S_H$  transition occurs. Figures 9 and 11 clearly show the deviation between the  $K_1$ – $K_2$  line and dotted curve at higher pressures. This indicates that applying pressure enlarges the deviation of molecular reorganization of the  $K_2$  crystal between the molecular and lateral chain directions. The molecular rearrangement of PB-18 at 300–400 MPa occurs first by chain extension during the  $K_1$ – $K_2$  transition. Merging of wide-angle reflections occurs consecutively and then lateral packing in the  $K_2$  crystal becomes loose at higher temperatures. The structural behavior of PB-18 is common in PB-14 and PB-16 polyesters. This phenomenon of PB-14–PB-18 under high pressure is apparently different from those of PB-10 and PB-12: in fact, PB-10 and PB-12 do not show the  $K_2$  phase at high temperatures. From the point of lateral ordering, the trend of a narrowing pretransition region in the  $K_1$  phase with pressure is clearly seen in PB-10 and -12, while the pretransition region in the  $K_2$  phase is almost constant in PB-14–PB-18. Pressure contributes remarkably to the narrowing of the  $K_1$ – $K_2$  transition and also to the deviation of molecular rearrangement in the lateral chain direction to that in the molecular chain direction.

**Table 1.** Long  $d$  Spacing for the Even-Membered Series of the PB- $n$  Polyesters

$P$ /MPa	type of phase	long $d$ spacing/Å <sup>b</sup>				
		PB-10	PB-12	PB-14	PB-16	PB-18
0.1 <sup>a</sup>	$K_1$	21.4	23.0	24.7	26.3	28.0
	$K_2$			25.5	27.5	29.4
	$S_H$	18.9	21.0	23.1	25.2	27.3
100	$K_1$	20.9	22.6	24.2	26.0	27.9
	$K_2$			25.6	27.1	30.3
	$S_H$	18.6	( $S_B$ 26.9)	23.0	24.9	27.5
200	$K_1$	20.8	22.3			27.7
	$K_2$					29.7
	$S_H$	18.6	( $S_B$ 26.5)			27.4
300	$K_1$	20.8	22.1	23.3		27.3
	$K_2$			24.2		29.3
	$S_H$	18.6	( $S_B$ 26.2)	22.4		27.1

<sup>a</sup> Data at 0.1 MPa (atmospheric pressure) are averaged by least-squares regression. <sup>b</sup> Errors in  $d$  spacings are within  $\pm 0.1$  Å.

Table 1 exhibits the variation of the  $d$  spacing estimated from the low-angle reflection of a homologous series of PB- $n$  polyesters. As one can see in Table 1, the long  $d$  spacing of the  $S_H$  phase is slightly dependent on pressure for all PB- $n$  polyesters, except PB-12. The tilt angle of the PB- $n$  molecule with respect to the layer normal is estimated to be approximately 38–40° in the  $S_H$  phase, showing a small pressure dependence. On the other hand, one can see a substantial compression of the long  $d$  spacing of the  $K_1$  crystal for PB-14 and PB-18. Such a strange phenomenon may be attributed to the change in molecular arrangement in which the tilt angle of the molecule in the  $K_1$  crystal is varied from 31.5° to 35° for PB-12, from 33° to 38° for PB-14, and from 36° to 39° for PB-18 by applying pressure, respectively.

Fluorescence measurements of PB-10 on heating show the shift of peak wavelength in fluorescence excited at 320 nm.<sup>24</sup> It is reduced to the change of molecular interaction between mesogenic moieties; i.e., the interaction between the fully overlapping biphenyl groups in the  $K_1$  crystal changes to a coplanar interaction between a biphenyl group and an ester moiety. In fluorescence spectra, the temperature dependence of the fluorescence peak wavelength shows a common break at 175 °C, suggesting the occurrence of some transition. The  $T$  point in this study seems to correspond to the change of microstructure obtained by the fluorescence measurement. Structural analysis of the PB-18 polyester by <sup>13</sup>C solid state NMR spectroscopy is underway to analyze the detailed structures of the  $K_1$ ,  $K_2$ , and  $S_H$  phases. Recently, it was found that there is a remarkable difference in the conformation of mesogenic moieties and packing structure: the  $K_1$  crystal has a coplanar conformation of the biphenyl moieties, while the  $K_2$  crystal has a twisted conformation of the biphenyl moieties and is nearly coplanar with the ester bond.<sup>25</sup> Since crystal structures of PB- $n$  polyesters are not determined definitely, the study on the phase transformation of PB- $n$  polyesters is still an interesting theme.

## Concluding Remarks

The structural behavior of a homologous series of PB- $n$  thermotropic polyesters with an alternate arrangement of 4,4'-dihydroxybiphenyl as a mesogen and alkanedioic acid as a flexible spacer was studied by WAXD experiments under hydrostatic pressures up to 300 MPa. As Krigbaum and Watanabe<sup>6,7</sup> reported in the results of these polyesters at atmospheric pressure, the same  $K_1$ – $S_H$ –I transition in PB-8 and -10 occurs

reversibly in the whole pressure region.<sup>17</sup> PB-12 exhibits the same transition process at pressures below 100 MPa, while a pressure-induced  $S_B$  mesophase appears in place of the  $S_H$  phase at higher pressures. If one adopts the merging point of wide-angle reflections as the midpoint of the  $K-S_H$  transition, one can discuss further the pressure dependence of the  $K_1-S_H$  and  $K_2-S_H$  transition processes of PB- $n$  polyesters.

PB- $n$  polyesters with long spacers of  $n \geq 14$  exhibit another crystal polymorph ( $K_2$ ) between the  $K_1$  and  $S_H$  phases, and they show reversibly the  $K_1-K_2-S_H-I$  phase transition at pressures up to 300 MPa. The long  $d$  spacing increases gradually by about 1–2 Å with temperature during a broad  $K_1-K_2$  transition on heating. The longer  $d$  spacing of the  $K_2$  phase shrinks discontinuously by 1.0–2.9 Å at the  $K_2-S_H$  transition, depending upon hydrostatic pressure. It is noteworthy that both the  $K_1$  and  $K_2$  crystals are deformed substantially in the molecular chain direction by applying pressure, in contrast to a slight change in the  $d$  spacing of the  $S_H$  phase. Deformation of these phases in the chain direction is on the order of  $K_2 > K_1 > S_H$ . It is found that the compressional behavior of long spacing for the two phases results in comparable values of  $d$  spacing between the  $K_1$  crystal and the  $S_H$  phase at high pressures (300–400 MPa).

## References and Notes

- (1) Keyes, P. H.; Weston, H. T.; Daniels, W. B. *Phys. Rev. Lett.* **1973**, *31*, 628.
- (2) Lin, W. J.; Keyes, P. H.; Daniels, W. B. *Phys. Lett.* **1974**, *49A*, 453.
- (3) Cladis, P. E.; Goodby, J. W. *Mol. Cryst. Liq. Cryst.* **1982**, *72*, 307.
- (4) Cladis, P. E.; Goodby, J. W. *Mol. Cryst. Liq. Cryst.* **1982**, *72*, 313.
- (5) Asrar, J.; Toriumi, H.; Watanabe, J.; Krigbaum, W. R.; Ciferri, A. *J. Polym. Sci., Polym. Phys. Ed.* **1983**, *21*, 1119.
- (6) Krigbaum, W. R.; Watanabe, J.; Ishikawa, T. *Macromolecules* **1983**, *16*, 1271.
- (7) Watanabe, J.; Krigbaum, W. R. *Macromolecules* **1984**, *17*, 2288.
- (8) Maeda, Y.; Mabuchi, T.; Watanabe, J. *Thermochim. Acta* **1995**, *266*, 189.
- (9) Chandrasekhar, S.; Ramaseshar, S.; Reshamwala, A. S.; Sadashiva, B. K.; Shashidhar, R.; Surendranath, V. *Liq. Cryst. Proc. Int. Conf.* **1975**, *1*, 117.
- (10) Chandrasekhar, S.; Shashidhar, R. In *Advances in Liquid Crystals*; Brown, G. H.; Academic Press: New York, 1979, Vol. 4, 2.
- (11) Spratte, W.; Schneider, G. M. *Mol. Cryst. Liq. Cryst.* **1979**, *51*, 101.
- (12) Hartmann, M.; Jenau, M.; Würflinger, A.; Godlewska, M.; Urban, S. *Z. Phys. Chem.* **1992**, *177*, 195.
- (13) Rübesamen, J.; Schneider, G. M. *Liq. Cryst.* **1993**, *13*, 711.
- (14) Hsiao, B. S.; Shaw, M. T.; Samulski, E. T. *Macromolecules* **1988**, *21*, 543.
- (15) Hsiao, B. S.; Shaw, M. T.; Samulski, E. T. *J. Polym. Sci., Polym. Phys. Ed.* **1990**, *28*, 189.
- (16) Maeda, Y.; Blumstein, A. *Mol. Cryst. Liq. Cryst.* **1991**, *195*, 169.
- (17) Maeda, Y.; Tanigaki, N.; Blumstein, A. *Mol. Cryst. Liq. Cryst.* **1993**, *237*, 407.
- (18) Maeda, Y.; Toriumi, H. *Makromol. Chem.* **1993**, *194*, 3123.
- (19) Maeda, Y.; Watanabe, J. *Macromolecules* **1993**, *26*, 401.
- (20) Maeda, Y.; Watanabe, J. *Macromolecules* **1995**, *28*, 1661.
- (21) Gray, G. W.; Goodby, J. W. G. *Smectic Liquid Crystals*; Leonard Hill: Glasgow, Scotland, 1984; Chapters 2, 5, and 8.
- (22) Maeda, Y.; Kanetsuna, H. *Bull. Res. Inst. Polym. Text.* **1985**, *149*, 119.
- (23) Maeda, Y. *Thermochim. Acta* **1990**, *163*, 211.
- (24) Huang, H. W.; Horie, K.; Yamashita, T.; Machida, S.; Sone, M.; Tokita, M.; Watanabe, J.; Maeda, Y. *Macromolecules* **1996**, *29*, 3485.
- (25) Sone, M. Private communication, 1996.

MA970052H